JOURNAL OF APPLIED ELECTROCHEMISTRY 20 (1990) 125–131

Impedance spectroscopy of the Ti(IV)/Ti(III) redox couple in the molten LiCl–KCl eutectic melt at 470° C*

D. M. FERRY, G. S. PICARD

Laboratoire d'Electrochimie Analytique et Appliquée (U.A. 216 du CNRS) Ecole Nationale Supérieure de Chimie de Paris, 11 rue P. et M. Curie, 75231 Paris Cedex 05, France

Received 8 February 1989

The electrochemical oxidation of Ti^{3+} ions in LiCl–KCl eutectic melt at 470° C occurs in two different ways according to the current densities. In our experimental conditions (concentration of Ti^{3+} ions 0.11 mol kg^{-1}) for potentials lower than -0.48 V (vs chlorine electrode) and current densities lower than 10 mA cm^{-2} soluble Ti^{4+} ions are formed, whereas, for higher potentials solid K_2TiCl_6 precipitates at the electrode resulting in a partial passivation of the electrode. Both reactions have been studied by means of impedance measurements which have shown the reversibility of the electrochemical reaction ($k_0 = 0.25$ cm s^{-1}; $\alpha = 0.3$) and the porosity of the K_2TiCl_6 layer electrochemically formed. The thickness of this layer has been estimated from the amount of electricity involved in the reaction and from the resistance and the capacitance characterising the deposit, measured at high frequencies. This comparison shows that the deposit is composed of a very thin (~ 0.1 μm) barrier layer covered by a very thick (~ 70 μm) porous external layer.

1. Introduction

This paper deals with the electroanalysis of the Ti(IV)/Ti(III) redox couple in the molten LiCl–KCl eutectic melt at 743 K. The study is a part of a systematic investigation into the possibility of using molten salts for titanium extractive metallurgy. In our previous papers [1–3] we have shown, by studying the acidic properties of titanium chlorides, that titanium ores (rutile and ilmenite) can be chlorinated in molten chlorides at low temperature (about 500° C) by using chlorinating gaseous agents in order to obtain a titanium (IV) solution which can further be electrolysed to produce high-purity titanium metal.

We have also studied the redox properties of Ti(III)/Ti(II) and Ti(II)/Ti(O) systems in order to have at our disposal fundamental data for the last stage of this molten salt process. A good knowledge of the Ti(IV)/Ti(III) redox couple is also needed both within the framework of this low temperature molten salt process and the electrolysis of $TiCl_4$ resulting from the Kroll process.

In a previous study [2] we have shown, by several electrochemical techniques, that the oxidation of Ti^{3+} into Ti(IV) occurs in a single reversible step. The Ti(IV) solubility was determined as being equal to $(4 \pm 1) \times 10^{-2}$ mol kg^{-1}. According to Mui and Flengas [14] this solubility is due to the precipitation of the solid compound K_2TiCl_6 which is in equilibrium with a partial pressure of gaseous $TiCl_4$ at a given temperature (for example 0.45 atm at 470° C). The sampled current voltammogram of Fig. 1 [2] shows that precipitation of titanium (IV) does not occur for potentials lower than -0.48 V (corresponding to current densities lower than 10 mA cm^{-2}). The oxidation of Ti(III) then corresponds to the reaction:

$$Ti^{3+} - e^- \leftrightarrow Ti^{4+} \quad (1)$$

For higher potentials the formation of a titanium (IV) compound deposit is experimentally observed. The reaction is then:

$$Ti^{3+} - e^- + 2K^+ + 6Cl^- \leftrightarrow K_2TiCl_6(s) \quad (2)$$

The purpose of this paper is to confirm and clarify these results, especially by means of impedance measurements performed in both regions of potential.

2. Experimental

2.1. *Apparatus and preparation of the melt*

The eutectic mixture (58.8 mol % LiCl–41.2 mol % KCl, analytical grade Merck) was melted in a Pyrex crucible placed inside a Pyrex reactor within a Renat furnace and then kept under a dry argon atmosphere. The temperature was controlled by a Gulton 3200 self-tuning controller. Solid titanium (III) chloride (purity > 99%) from Alpha Ventron was used because of its high solubility in the melt and its easy handling compared with those of $TiCl_4$. It was kept in a dry glove box before its introduction to the cell by means of a 'powder burette', as described in [5].

* Paper presented at the EUCHEM Conference on Molten Salts 1988, St Andrews, Scotland, 6 July 1988.

0021-891X/90 $03.00 + .12

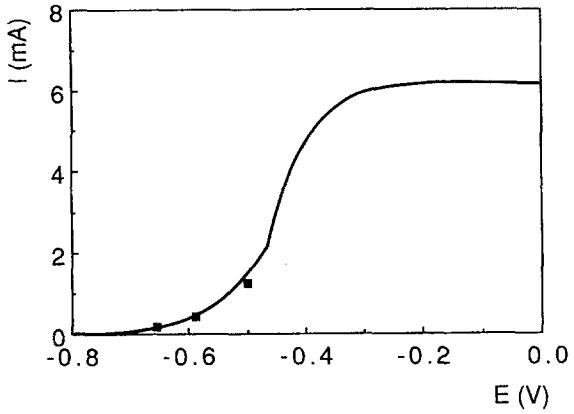

Fig. 1. ——, Sampled-current voltammogram of the oxidation of Ti^{3+} ions (0.11 mol kg^{-1}) into Ti(IV). Working electrode: tungsten. $S = 0.24\,cm^2$. After [2]. ■, currents measured with our impedance device (this study).

2.2. *Electrodes*

The working and counter electrodes were tungsten wires supplied by Johnson Matthey ($\phi = 0.5$ mm). The silver–silver chloride (0.75 mol kg^{-1}) system was used for the reference electrode. The potential of this electrode is -1.023 V vs Cl^-/Cl_2 (1 atm). All the potentials given in this paper are referred to the chlorine electrode.

2.3. *Electrochemical techniques*

Chronoamperograms were recorded by using an EG&G-PAR Model 176 potentiostat–galvanostat connected to an Apple II microcomputer via a Model 273 interface. AC impedance measurements were performed with a Tacussel Z computer system coupled to a Hewlett-Packard 9826A microcomputer. Data were analysed by using an HP 9000 'Series 300' microcomputer.

3. Results and discussion

3.1. *Studies in the potential range ($E < 0.48$ V) where Ti(IV) is soluble*

Experimental measurements were performed at -0.64, -0.59 and -0.49 V. The steady-state current values which were measured by the impedance device are in good agreement (Fig. 1) with those obtained previously [2]. Impedance data are reported in the Nyquist and Bode planes on Fig. 2. These spectra exhibit a capacitive loop at high frequencies corresponding to the charge transfer and, for low frequencies, a straight line with slope unity indicating a Warburg diffusional behaviour. This is confirmed by plotting the real and imaginary parts of the electrochemical impedance versus the reciprocal of the square root of the angular frequency (Fig. 3). We obtained two parallel straight lines, which is characteristic of a diffusional impedance.

The impedance spectra were computerized by means of the simple reaction model (1) involving two mass transfer steps (diffusions of Ti(III) and electro-

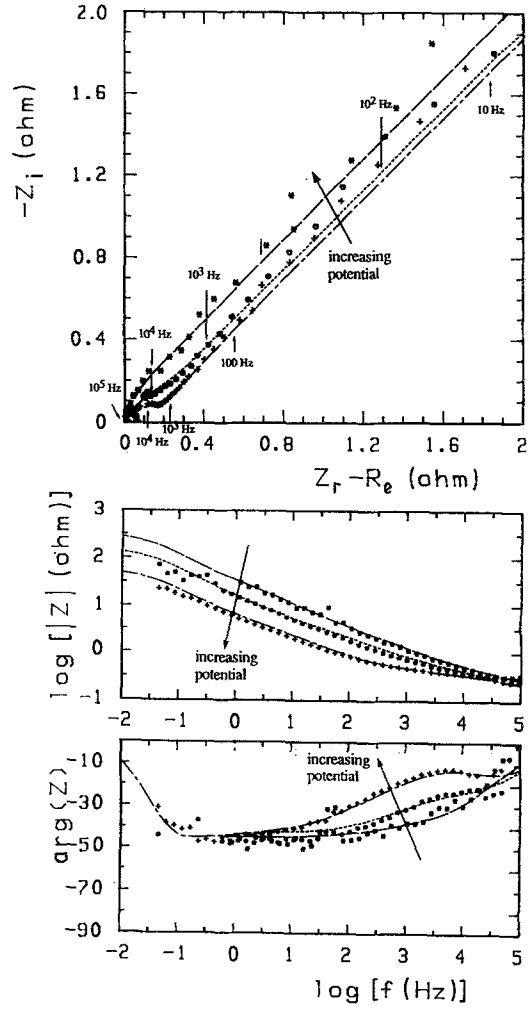

Fig. 2. Nyquist and Bode plots and corresponding simulated curves. Applied potentials, -0.64, -0.59, -0.49 V.

chemically produced Ti(IV)) and one electron transfer step. The corresponding electrical equivalent circuit is shown in Fig. 4. R_u is the uncompensated resistance of the bath, C_d the double layer capacitance, R_{ct} the charge transfer resistance and W the Warburg diffusion impedance. R_{ct} is related to the kinetic constants of the model by the equation [6]:

$$1/R_{ct} = nFS(k_f b_f C_{re} + k_b b_b C_{oe}) \quad (3)$$

where F is the Faraday constant, S the area of the electrode, C_{re} and C_{oe} the respective concentrations of Ti^{3+} and Ti^{4+} ions at the electrode and k_f and k_b the rate constants of the oxidation and reduction reactions. These constants are given by:

$$k_f = k_0 \exp[-b_f(E - E_0)] \quad (4)$$

$$k_b = k_0 \exp[-b_b(E - E_0)] \quad (5)$$

where k_0 and E_0 are, respectively, the intrinsic rate constant and the standard potential of the electrochemical reaction. We have also:

$$b_f = \alpha nF/RT \quad (6)$$

$$b_b = (1 - \alpha)nF/RT \quad (7)$$

where α is the charge transfer coefficient, R the gas constant and T the temperature in Kelvin. The diffusion

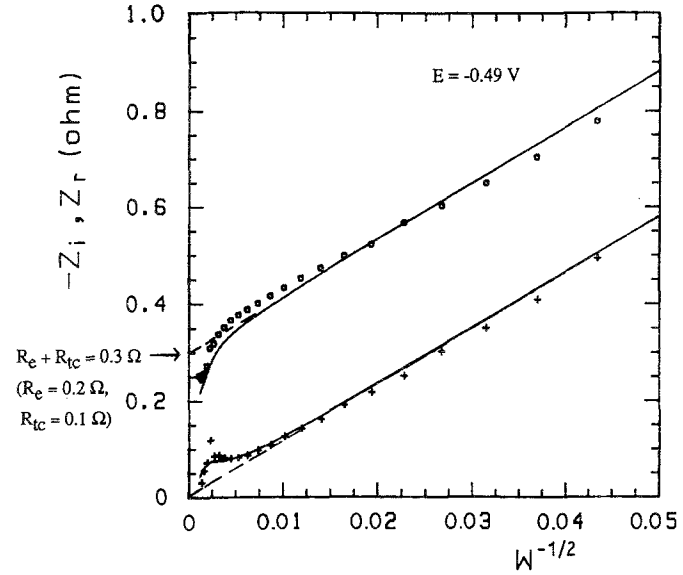

Fig. 3. Randles impedance diagram showing the diffusional behaviour of the studied system. Applied potential, −0.49 V.

impedance W is given by the following expression [7]:

$$W = R_{ct}(k_f + k_b)\frac{\text{th}\,(j\omega\delta/D)^{1/2}}{(j\omega\delta)^{1/2}} \qquad (8)$$

where ω is the angular frequency, D the diffusion coefficient of Ti^{3+} and Ti^{4+} ions (assumed equal for both ions knowing that the solvated ions $TiCl_6^{3-}$ and $TiCl_6^{2-}$ have the same octohedral structure [8]) and δ the thickness of the diffusion layer. The simulated curves obtained by using this model are represented as solid lines on the Nyquist, Bode and Randles plots of Figs 2 and 3. We obtained a good fit by using the values determined previously [2] for the standard potential E_0, D and δ by taking the following values for k_0 and α:

$$k_0 = 0.25\,\text{cm s}^{-1}$$
$$\alpha = 0.3$$

The double layer capacitance C_d and the uncompensated resistance of the bath R_u were also determined. We have obtained:

$$C_d = 125\,\mu\text{F cm}^{-2}$$
$$R_u = 0.06\,\Omega\,\text{cm}^2$$

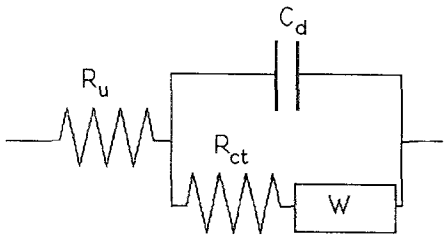

Fig. 4. Equivalent electrical circuit of the simple mechanism used (see text) to simulate experimental impedance diagrams. R_u, uncompensated resistance of the electrolyte. R_{ct}, charge transfer resistance. C_d, double layer capacitance. W, Warburg diffusional impedance.

3.2. *Analysis of data resulting from a study in the potential range ($E > 0.48$ V) where Ti(IV) precipitates as K_2TiCl_6*

3.2.1. Time dependence of the faradaic current. For higher values of potential we observed that the current, measured after the onset of the potential, decreases and that a relaxation time of more than 12 min was necessary to reach a steady-state value (curves 4, 5, 6, 7 and 8 of Fig. 5a), contrary to what was observed for lower potentials (curves 1, 2 and 3 of Fig. 5a). The sampled current voltammogram obtained with a sample time of 20 min exhibits a limiting current (i_2) lower than that one obtained (i_1) with a shorter sample time (20 s) (Fig. 5b). This phenomenon may be attributed to a decrease of the active electrode area due to the insulating character of the K_2TiCl_6 deposit. This active area S_{act} can be calculated from the initial one S_0 by the relation:

$$S_{act} = S_0\frac{i_2}{i_1} \qquad (9)$$

Experimentally we obtained $i_1 = 6.3$ mA and $i_2 = 2.5$ mA. Using the value of S_0 (0.24 cm^2) we have:

$$S_{act} = 0.1\,\text{cm}^2$$

This area remains constant after a certain time of electrolysis because of a formation-dissolution process of the precipitate layer. K_2TiCl_6 is formed at the electrode with a rate proportional to the faradaic current, whereas it dissolves at a constant rate k_d. The variation of the thickness e of the deposit is then given by the relation:

$$e(t) = \int_0^t i\frac{M}{FdS}\,dt - k_d\frac{M}{dS}\,dt \qquad (10)$$

where M is the molecular weight of K_2TiCl_6 and d the density of this compound. For long times a steady

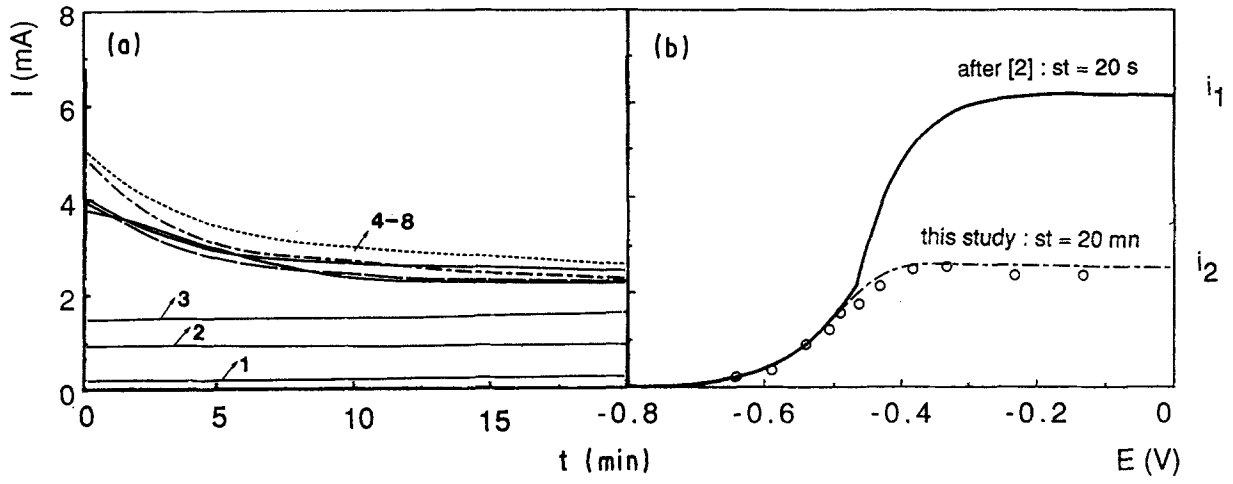

Fig. 5. (a) Chronamperograms recorded at various potentials during the impedance measurements. 1–3, potentials at which no precipitation of K_2TiCl_6 occurs. 4–8, potentials at which precipitation occurs. (b) Corresponding sampled-current voltammograms for short (st = 20 s, after [2]) or long (st = 20 min) sample time.

state current is reached $i_{st} = k_d F$ corresponding to a constant value of the layer thickness. Transiently, the thickness is thus given by:

$$e(t) = \frac{M}{FdS}\left(\int_0^t i\,dt - i_{st}\int_0^t dt\right) \qquad (11)$$

This thickness is then proportional to the quantity of electricity Q represented by the hatched area on Fig. 6.

Experimentally we have (for potentials ranging from −0.44 to −0.14 V) $Q = 0.48 \pm 0.12$ C. The thickness e has been calculated by using a value for d estimated from those of similar compounds (K_2SnCl_6, K_2ReCl_6, K_2PtCl_6, K_2PdCl_6). In fact the ratio d/M is almost constant and equal to 6.9×10^{-3} cm^{-3} for all these compounds.

$$d(K_2TiCl_6) = 2.35\,\text{g cm}^{-3}$$
$$e = 30 \pm 8\,\mu\text{m}$$

This value assumes the formation of a compact deposit on a plane surface, but the real value may be different because of the porosity of the deposit, as will be seen later.

3.2.2. Impedance spectra analysis. Experimental data obtained by impedance spectroscopy in the potential range where titanium (IV) precipitates are reported in Fig. 7. Firstly, it is seen that the capacitive loop observed at high frequencies increases with the applied potential. Secondly the slope of the straight line observed for low frequencies decreases with the applied potential (Fig. 7a, b). The Bode phase plot shows that the phase angle at low frequencies takes a constant value close to 20° (Fig. 7c). This may be characteristic of a diffusion process through a porous layer [9]. For high potentials ($E \geqslant -0.24$ V) the phase angle (at low frequencies) seems to increase again. This phenomenon is also noticeable on the Nyquist plots (Fig. 7b).

We have seen that the high frequency capacitive loop increases with the applied potential. The size of this loop has been compared to that expected from the potential dependence of the charge transfer resistance. For that purpose we measured the high frequency resistance R directly from the Nyquist diagrams by comparing this part of the diagrams to a semi-circle (Fig. 8a). The corresponding high frequency capacitance has been determined from the relation:

$$Z_i = -\frac{1}{2\pi fC} \qquad (12)$$

By plotting $\log(-Z_i)$ versus $\log(f)$ for high frequency values we experimentally obtained a straight

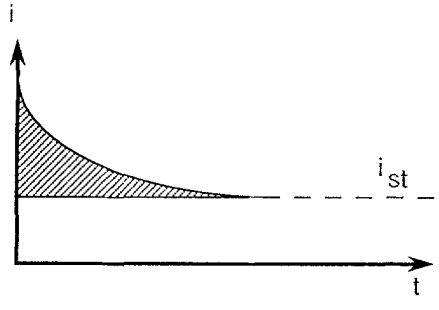

Fig. 6. The quantity of electricity corresponding to the quantity of K_2TiCl_6 deposited onto the electrode after a steady state is reached.

Table 1. Values of the high frequency resistance R and capacitance C as a function of the applied potential (in the range where precipitation of K_2TiCl_6 occurs) and corresponding time constant (product RC)

E (V)	C (μF)	R (Ω)	RC (μS)
−0.46	19.1	0.6	11.5
−0.44	6.6	1.8	11.9
−0.39	2.5	4.7	11.7
−0.34	2.1	5.6	11.8
−0.24	1.7	7.0	11.9
−0.14	0.8	14.8	11.8

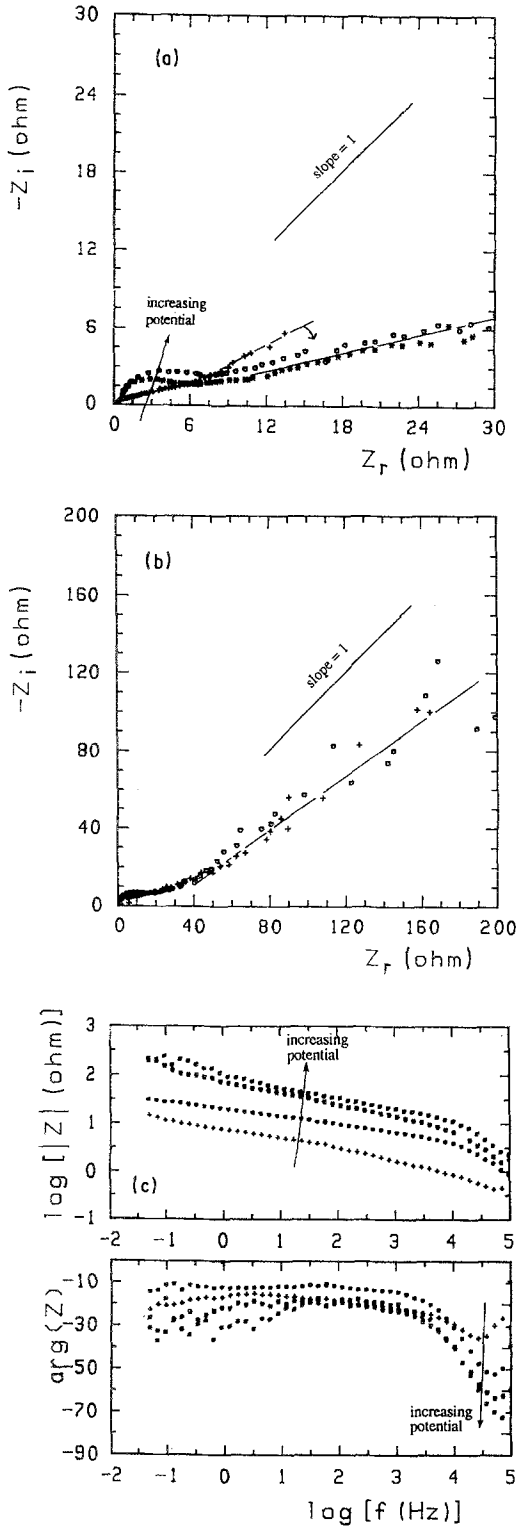

Fig. 7. (a) Nyquist diagrams obtained at −0.465, −0.39 and −0.34 V. (b) Nyquist diagrams obtained at −0.24 and −0.14 V. (c) Bode plots obtained at −0.465, −0.39, −0.24 and −0.14 V.

line with a slope of unity (Fig. 8b). At the frequency f_0 for which $\log(-Z_i) = 0$, we have:

$$C = \frac{1}{2\pi f_0} \tag{13}$$

The values of R and C so obtained are given in Table 1. It is seen that the product RC is constant whatever the applied potential and equal to 11.8 ± 0.1 μs. This is confirmed by the plots of $-Z_i$ versus frequency (Fig. 9) that exhibits a maximum for a fairly

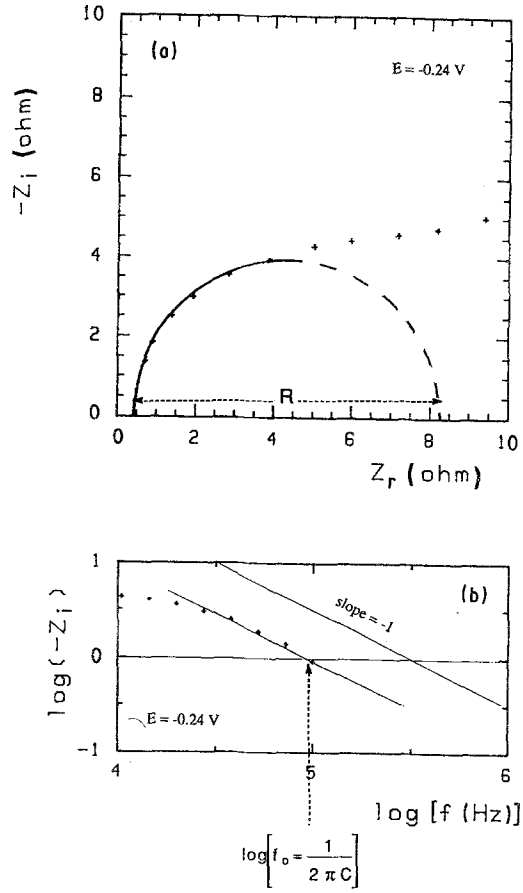

Fig. 8. (a) Comparing the high frequency part of the Nyquist plot to a semi-circle. (b) Variation of the logarithm of the opposite imaginary part of the impedance as a function of the logarithm of the frequency.

constant frequency values f_m close to $10^{4.13}$ Hz. The formula $RC = 2\pi f_m$ gives, for the product RC, the same value as the preceeding one. This suggests that we are measuring the impedance of the porous precipitated layer K_2TiCl_6. In fact, concerning the charge transfer itself, the calculated time constant $R_{ct}C_d$ should increase with potential, as shown in Fig. 10a. The corresponding frequency should then decrease with potential as shown in Fig. 10b. This is probable because the R_{ct}–C_d circuit is hidden by the R–C circuit of the layer itself (Fig. 11).

3.3. *Porous layer model for electrochemically precipitated K_2TiCl_6*

It is possible to estimate the layer thickness e from the

Table 2. Values of the thickness of the K_2TiCl_6 deposit as a function of the applied potential considering the geometrical (S_{geom}) and the active (S_{act}) area of the electrode

E (V)	estimated e (Å) ($S = S_{geom}$)	estimated e (Å) ($S = S_{act}$)
−0.46	1.1– 110	0.46– 46
−0.44	3.3– 330	1.4 – 140
−0.39	8.6– 860	3.6 – 360
−0.34	9.3– 930	3.9 – 390
−0.24	12.8–1280	5.3 – 530
−0.14	27.1–2710	11.3 –1130

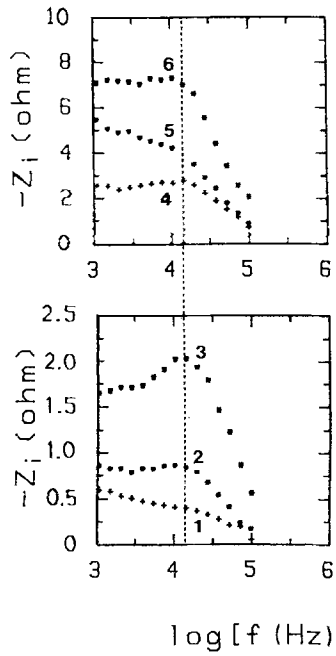

Fig. 9. Variation of the opposite imaginary part of the impedance as a function of the logarithm of the frequency.

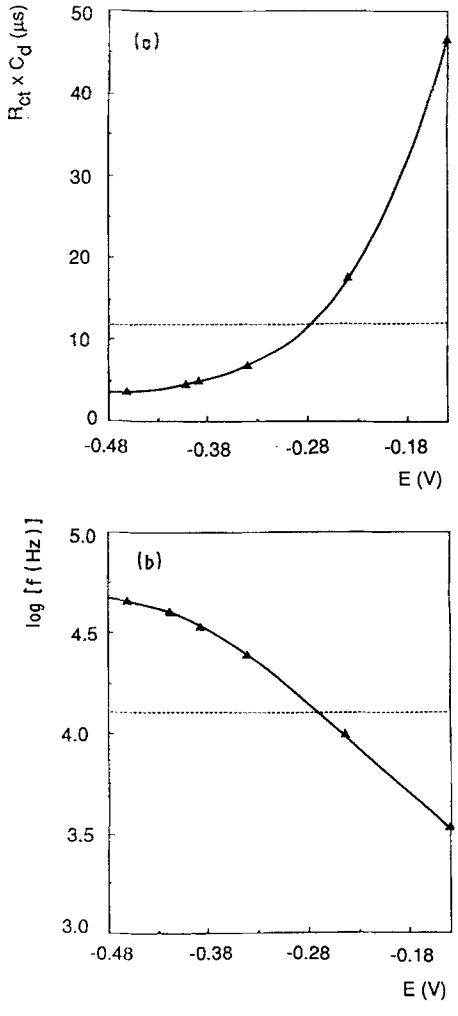

Fig. 10. Variations of (a) the expected time constant $R_{ct}C_d$ and (b) the corresponding frequency, as a function of the applied potential (▲, experimental potentials). ----, value experimentally measured at high frequency.

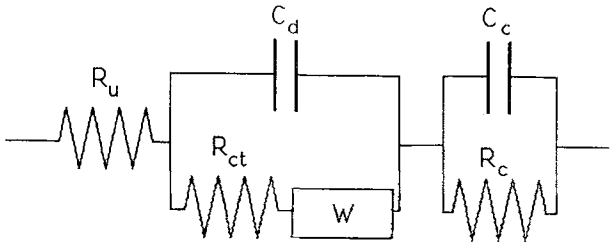

Fig. 11. Equivalent electrical circuit of the electrode–electrolyte interface taking into account the layer of K_2TiCl_6. (C_c, capacitance of the layer; R_c, resistance of the layer).

preceeding data by one of the following formulae:

$$e = RS/\varrho \quad (12)$$

$$e = \varepsilon_0 \varepsilon_r S/C \quad (13)$$

where ϱ represents the resistivity of the solid compound (K_2TiCl_6), ε_r its relative permittivity and ε_0 the permittivity of free space. ε_r ranges from 10 to 1000 for such a compound [10] and the resistivity ϱ can be estimated from the relation:

$$\varrho = RC/\varepsilon_0 \varepsilon_r \quad (14)$$

The value must lie in the range 1.3×10^7 to 1.3×10^5 Ω cm (this value corresponds to a poorly conducting compound which confirms the passivating character of the layer). The thicknesses so calculated, and assuming the electrode area to be equal to its geometrical area, are given in column 1 of Table 2. We can see that these values (at the most 0.27 μm) are considerably smaller than that (30 ± 8 μm) calculated from the amount of electricity involved in the electrochemical reaction. This may be due to the heterogeneity of the layer, the electrode being covered on its 'active' area by a very thin 'barrier' layer of the precipitated compound, whereas the most important part of the deposit forms a very thick porous external layer partially 'blocking' the electrode (Fig. 12). Such a model has been recently developed by Vereecken *et al.* [11] in the case of alumina layers onto aluminium. The real thickness of the barrier layer must then be calculated by considering the active area of the electrode (Table 2, column 2). Figure 13 shows that the maximum thickness so calculated increases with potential in a rather linear way, as previously noticed by Vereecken *et al.*. If we consider that the quantity of material deposited onto the electrode is essentially concentrated inside the porous external layer (that of the barrier layer being negligible), it is then possible to calculate the depth of the pores by the expression:

$$l = e \frac{S_0}{S_{act}} \quad (15)$$

where e is the thickness of the equivalent compact deposit (30 μm). We find $l = 72$ μm.

4. Conclusion

In this paper we have shown, by using impedance spectroscopy, that Ti^{3+} ions can be oxidized to partially

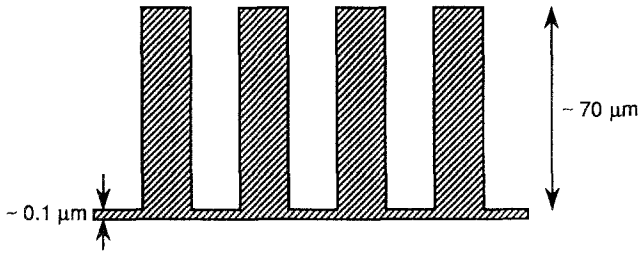

Fig. 12. Schematic diagram of the porous layer of K_2TiCl_6.

soluble Ti(IV) in a single reversible step. When the solubility of Ti(IV) is reached a porous layer of K_2TiCl_6 is formed on the electrode. The insulating character of this compound induces a partial passivation of the electrode whereas the 'active' area of the electrode is covered by a very thin 'barrier' layer allowing the flow of current.

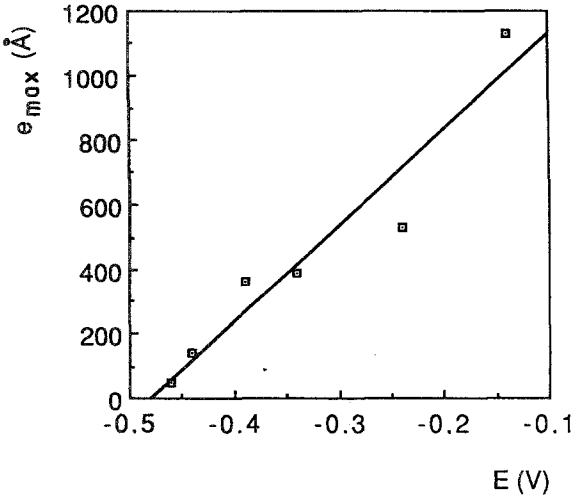

Fig. 13. Variation of the maximum value of the thickness of the barrier layer as a function of the applied potential.

Acknowledgement

We are grateful to Professor B. Trémillon for his interest in this work.

References

[1] D. Ferry, E. Noyon and G. Picard, *J. Less common Metals* **97** (1984) 331.
[2] D. M. Ferry, G. S. Picard and B. L. Tremillon, *J. Electrochem. Soc.* **135** (1988) 1443.
[3] D. M. Ferry, G. S. Picard and B. Tremillon, *Trans Instn Min. Metall. Sect. C* **97** (1988) C21.
[4] J. H. Mui and S. N. Flengas, *Can. J. Chem.* **10** (1962) 997.
[5] F. Seon, G. Picard and B. Tremillon, *Electrochim. Acta* **28** (1983) 209.
[6] A. J. Bard and L. R. Faulkner, in 'Electrochemical Methods, Fundamentals and Applications', John Wiley, New York (1980).
[7] E. Warburg, *Wied. Ann* **67** (1899) 493; *Drud. Ann* **6** (1901) 125.
[8] E. Chassaing, F. Basile and G. Lorthioir, in 'Titanium '80, Science and Technology', Proceedings of the 4th International Conference on Titanium, Kyoto, Japan, May, 19-22 (edited by H. Kimura and O. Izumi) (1980).
[9] R. de Levie, *Electrochim. Acta* **9** (1964) 1231.
[10] CRC Handbook of Chemistry and Physics, 69th edition, CRC Press (1988–89).
[11] J. Vereecken, H. Terryn, B. van der Linden, 'Comptes Rendus du 3ème Forum sur les Impédances Electrochimiques', Montrouge, France (1988).